APPLIED AND ENVIRONMENTAL MICROBIOLOGY, Oct. 2006, p. 6514–6526 Vol. 72, No. 10
0099-2240/06/$08.00+0 doi:10.1128/AEM.01066-06

Dissimilatory Arsenate and Sulfate Reduction in Sediments of Two Hypersaline, Arsenic-Rich Soda Lakes: Mono and Searles Lakes, California

T. R. Kulp,[1] S. E. Hoeft,[1] L. G. Miller,[1] C. Saltikov,[2] J. N. Murphy,[2] S. Han,[3] B. Lanoil,[3] and R. S. Oremland[1]*

U.S. Geological Survey, Menlo Park, California 94025[1]; Department of Environmental Toxicology, University of California at Santa Cruz, Santa Cruz, California 95064[2]; and Department of Environmental Sciences, University of California at Riverside, Riverside, California 92521[3]

Received 9 May 2006/Accepted 31 July 2006

A radioisotope method was devised to study bacterial respiratory reduction of arsenate in sediments. The following two arsenic-rich soda lakes in California were chosen for comparison on the basis of their different salinities: Mono Lake (~90 g/liter) and Searles Lake (~340 g/liter). Profiles of arsenate reduction and sulfate reduction were constructed for both lakes. Reduction of [^{73}As]arsenate occurred at all depth intervals in the cores from Mono Lake (rate constant [k] = 0.103 to 0.04 h^{-1}) and Searles Lake (k = 0.012 to 0.002 h^{-1}), and the highest activities occurred in the top sections of each core. In contrast, [^{35}S]sulfate reduction was measurable in Mono Lake ($k = 7.6 \times 10^{-4}$ to 3.2×10^{-6} h^{-1}) but not in Searles Lake. Sediment DNA was extracted, PCR amplified, and separated by denaturing gradient gel electrophoresis (DGGE) to obtain phylogenetic markers (i.e., 16S rRNA genes) and a partial functional gene for dissimilatory arsenate reduction (*arrA*). The amplified *arrA* gene product showed a similar trend in both lakes; the signal was strongest in surface sediments and decreased to undetectable levels deeper in the sediments. More *arrA* gene signal was observed in Mono Lake and was detectable at a greater depth, despite the higher arsenate reduction activity observed in Searles Lake. A partial sequence (about 900 bp) was obtained for a clone (SLAS-3) that matched the dominant DGGE band found in deeper parts of the Searles Lake sample (below 3 cm), and this clone was found to be closely related to SLAS-1, a novel extremophilic arsenate respirer previously cultivated from Searles Lake.

Contamination of drinking water sources with naturally occurring arsenic (As) is a widespread environmental concern that affects the health of millions of people worldwide (25, 44). This problem has inspired considerable research into the biogeochemical processes that control the distribution and mobilization of As in aqueous environments. In sediments and subsurface aquifers, the mobility of As is controlled in part by the selective tendency of its oxyanions to adsorb onto the surfaces of common mineral phases of iron, manganese, and aluminum (37, 47, 53). The extent of this adsorption is highly dependent on the oxidation state and pH of the aqueous phase and on competition with other anions (e.g., phosphate and carbonate) for adsorption sites. Hence, studies on arsenic diagenetic behavior in sediments have been constrained by the difficulties associated with obtaining reliable chemical speciation data for the bulk arsenic associated with the solid phase (2, 22, 38, 43, 46). Although such speciation data can be obtained by sequential extraction procedures (13) or X-ray spectroscopy (14), the former approach is tedious, while the latter is subject to beam time availability. For these reasons, chemical and/or biological processes that could affect arsenic diagenesis in sediments are more easily studied in the water columns of stratified lakes and fjords (9, 27, 36, 40, 41).

A further complication of arsenic mobility in sediments is that the oxidation state of As can be controlled by microbially mediated transformations between its two most prevalent oxyanions, arsenate [As(V); $HAsO_4^{2-}$] and arsenite [As(III); $HAsO_2$] (24, 32, 33). While chemical (abiotic) reduction of As(V) with sulfide is possible, this reaction is highly pH dependent and occurs at significant rates only under strongly acidic conditions (5, 39). Thioarsenites themselves are insoluble at acidic to neutral pH values but are quite soluble under alkaline conditions (9, 50). Furthermore, the adsorption of As(V) is greatly diminished at high pH values (pH >8.5) (1, 37, 43). Arsenic mobility is also enhanced in phosphate-rich settings because phosphate competes directly for surface adsorption sites on sediment particles (4, 37).

For the reasons summarized above, soda lakes should be ideal laboratories to study arsenic sediment diagenesis because they are alkaline, have high carbonate contents, and contain elevated concentrations of phosphate. These factors, along with the extraordinarily high dissolved arsenic concentrations (from volcanic origins) in these lakes, have the effect of minimizing competing solid-phase chemical phenomena commonly encountered in circumneutral pH systems (34). This should result in association of the bulk of the As species present within the sediment matrix with the easily extracted pore waters rather than with the solid phase.

We have previously reported rates of arsenate and sulfate reduction in the anoxic water column of Mono Lake (ML)

* Corresponding author. Mailing address: U.S. Geological Survey, Menlo Park, CA 94025. Phone: (650) 329-4482. Fax: (650) 329-4463. E-mail: roremlan@usgs.gov.

TABLE 1. Some general chemical limnological characteristics of Mono Lake and Searles Lake brines[a]

Lake	pH	Salinity (g/liter)	Sulfate (*m*)[b]	$HCO_3^- + CO_3^{2-}$ (*m*)	Chloride (*m*)	Borate (*m*)	Sodium (*m*)	Phosphate (mM)	Arsenate (mM)
Mono	9.8	90	0.08	0.37	0.46	0.03	1.12	0.60[c]	0.20
Searles	9.8	310	0.73	0.63	5.25	0.46	7.43	20.0	3.9

[a] Data from multiple sources cited in references 29 and 30.
[b] Molality (*m*) = molarity/density of brine (Mono Lake, 1.09; Searles Lake, 1.31).
[c] Data from J. T. Hollibaugh (personal communication) and courtesy of the NSF-funded Mono Lake Microbial Observatory (MCB 99-77886).

obtained by employing the radiotracers [^{73}As]arsenate and [^{35}S]sulfate (27). In this study, we extended this approach to examine these processes in the littoral zone sediments of Mono Lake and Searles Lake (SL), both of which are in California. The former is a moderately hypersaline alkaline brine lake, while the latter is an alkaline brine lake that is fully salt saturated (29). We found that dissimilatory arsenate reduction (DAsR) can be detected at all depths sampled in both environments but that sulfate reduction occurs only in Mono Lake. The absence of detectable sulfate reduction in Searles Lake provides further support for the theory of Oren (35) concerning the exclusion of low-energy-yielding anaerobic processes (e.g., sulfate reduction and methanogenesis) from salt-saturated ecosystems. Moreover, we characterized the resident microbial flora in the sediments of each lake by employing PCR amplification and denaturing gradient gel electrophoresis (DGGE) separation of 16S rRNA gene fragments of the extracted DNA. We also obtained insight into the diversity of the microflora responsible for the DAsR activity observed by successful amplification and sequencing of the functional gene for respiratory ("dissimilatory") arsenate reductase (*arrA*) by employing primers previously used in freshwater ecosystems (18) that were modified by fitting with selective codons for halophilic archaea. Previous papers have reported the interaction of sulfate reduction and arsenate reduction determined in physiological studies performed with pure cultures (17, 24), in individually focused studies of novel *arrA* primer sets performed in anoxic aquatic environments (9, 18), or in studies of intensively measured metrics of sediment sulfate reduction (but not arsenate reduction) in numerous anoxic ecosystems over the past four decades. Hence, our work was a significant, interdisciplinary collaborative approach aimed at increasing our understanding of the biogeochemistry of arsenate and sulfate reduction in the sediments of two chemically comparable, but nonetheless unique, arsenic-rich ecosystems.

MATERIALS AND METHODS

Site description. Mono Lake and Searles Lake are located along the arid eastern escarpment of the Sierra Nevada mountain range in California. Selected geochemical and limnological characteristics of both lakes are summarized in Table 1. Dissolved constituents, including arsenic and sulfur compounds, are derived from weathering and input of hydrothermal fluids from the surrounding watersheds, and evaporative concentration of these constituents occurs in these terminal lakes. Mono Lake (mean depth, ~17 m) occasionally undergoes periods of meromixis resulting from density-controlled stratification of the water column (11). Searles Lake is a shallow, evaporated version of ML, and during the dry spring and summer months it is an evaporative saltern (depth, ~15 cm) that contains salt-saturated brine underlying a ~5-cm-thick salt crust. Precipitation runoff may accumulate in the SL basin during the wet winter months. At the time of sampling for this study (February 2005) the persistent salt crust and underlying brine were submerged beneath ~0.5 m of water, owing to the unusually high precipitation and runoff during the winter of 2004 and 2005.

Collection and processing of sediment cores. Duplicate hand cores (depth, 22 cm) were collected from the littoral zone sediments from the northeastern quadrant of ML (26) (38°04′27″N, 119°00′46″W) and from the sediments below the SL salt crust and brine (29) (35°42′38″N, 117°20′12″W). Mono Lake cores were processed in the field within 4 h after collection. Searles Lake cores were stored on ice during transport to the laboratory and were processed within 48 h after collection. During processing, cores were extruded vertically in a glove bag under an N_2 atmosphere and sectioned into 2- to 4-cm segments representing eight depth intervals along the length of the core (21, 30). Prior to further processing, subsamples (1 ml) for sediment porosity and pore water methane determinations were collected from each depth interval using 3-ml syringes with the hub end removed.

Porosity was calculated from the sediment water content (determined by weight loss on drying) using the relationship of Berner (3). The porosity of the ML core sediments ranged from 0.63 to 0.70 with depth, while the values were much lower for SL (0.19 to 0.35). The pore water density for each core segment was calculated from salinity measurements obtained with a Vista model A366ATC refractometer. The dry density of the sediment particles was assumed to be that of quartz (2.65 g/cm^3). The viscosities of ML and SL water were measured at 20°C using a capillary viscometer (International Research Glassware, Kenilworth, NJ). The downward flux of As(V) into the sediment from the overlying lake water was calculated using Fick's first law of diffusion: flux = $-\Phi D(\delta C/\delta Z)$, where Φ is the porosity of the topmost depth interval (0 to 2 cm), D is the sediment diffusion coefficient at 20°C corrected for viscosity ($\eta_{Mono} = 1.35 \times \eta_{water}$; $\eta_{Searles} = 5.20 \times \eta_{water}$) and tortuosity ($\theta^2_{Mono} = 1.54$; $\theta^2_{Searles} = 3.57$), C is the As(V) concentration, Z is the median sediment depth (1 cm) represented by the top interval, and $\delta C/\delta Z$ is the concentration gradient represented in the top interval [$D_{As(V)}$ (16) and tortuosity determination (48)].

Pore water analysis. Core segments from one core at each locality were transferred into hydrostatic "squeezers" to expel, filter, and collect pore fluids for geochemical analysis as described by Miller et al. (21). Filtered water samples were stored at 10°C in 10-ml Vacutainers prior to analysis. A 0.5-ml aliquot of pore water was added to a Vacutainer containing 1 ml of 10% zinc acetate to preserve the sample for sulfide analysis in the laboratory. Aqueous As(V) and As(III) contents of the pore water were determined by high-performance liquid chromatography–hydride generation atomic absorption spectroscopy (15, 19). Total arsenic contents were measured by hydride generation atomic absorption spectroscopy following microwave-aided oxidation to As(V) with $K_2S_2O_8$ and subsequent reduction to As(III) with 6 N HCl–10% KI (51). The concentration of As(III) present as arsenic sulfide compounds (thioarsenites) was calculated by determining the difference between the total As concentration and the sum of the concentrations of aqueous As(V) and As(III). Sulfide and ammonia contents were measured spectrophotometrically using the methods of Cline (6) and Solórzano (45), respectively. Sulfate, phosphate, and chloride contents were measured by ion chromatography (28). Methane contents were determined by extruding 1-ml sediment subsamples into 10-ml serum bottles with 2 ml of NaCl-saturated water, followed by shaking and analysis of headspace methane concentrations by flame ionization gas chromatography (31).

Radioassays for arsenate reduction and sulfate reduction. All manipulations of core sediment materials were performed in an N_2-filled glove bag. Core segments from the second duplicate core of each site were sampled for radioisotope experiments using methods adapted from the methods of Oremland et al. (27, 30, 31). Subcores (sediment volume, 2 ml) of each core section were taken using 3-ml plastic syringes with the hub end removed. The syringes containing sediment were then sealed with rubber stoppers and removed from the glove bag for injection of radioisotopes. We collected additional subcores from three segments of the Searles Lake core to serve as killed control samples, which were autoclaved twice (121°C, 250 kPa, 60 min) and then cooled to room temperature prior to injection.

Subcores for determining As(V) reduction were injected with 111 kBq $HNa_2{}^{73}AsO_4$ (100 μl; specific activity, 2,294 kBq/mmol; Brookhaven National Laboratory, Upton, NY). Subcores were incubated at 20°C for 28 h for SL samples and for 33 h for ML samples. At specified times during incubation, two duplicate subcores from each depth interval were frozen at −60°C to arrest activity until As extraction and analysis. We extracted ^{73}As from the subcores at each time by extruding the radiolabeled sediment plug from its syringe into 6 ml of 100 mM K_2HPO_4 and shaking the preparation on an orbital shaking table for 20 min to desorb and solubilize all radiolabeled As. The phosphate solution-sediment mixture was then centrifuged (500 × *g* for 25 min), and 200 μl of the supernatant was added to 2 ml of deionized water adjusted to pH 3. These 2.2-ml preparations were placed on ion-exchange columns (50- to 100-mesh AGI-X8 resin; Bio-Rad Laboratories, Hercules, CA) to separate dissolved $^{73}As(V)$ from its reduction products, $^{73}As(III)$ and [^{73}As]thioarsenite, as described by Oremland et al. (27). Samples were eluted with 30 ml of 0.12 N HCl to recover dissolved $^{73}As(III)$ and $^{73}As(V)$ and then with 30 ml of 1 M Na_2CO_3 to recover [^{73}As]thioarsenite. Arsenite eluted in the first 6 ml, whereas As(V) eluted in the subsequent 24 ml of HCl eluent. Eluted fractions were collected in scintillation vials, and counts were determined by gamma spectrometry. The counts recovered in the thioarsenite fraction were added to those obtained for the previously eluted As(III).

Subcores for determining sulfate reduction were injected with 370 kBq (for SL) or 703 kBq (for ML) $Na_2{}^{35}SO_4$ (100 μl; carrier free; American Radiolabeled Chemicals, Inc., St. Louis, MO) and incubated in the same way that the As(V) reduction subcores were incubated. Radiolabeled [^{35}S]sulfide produced by dissimilatory reduction of $^{35}SO_4$ was extracted and quantified at each time using methods described by Oremland and Miller (30). Briefly, the subcores were extruded into a sealed reaction vessel and reacted with 20 ml of a 1.0 M $CrCl_2$ solution in 6 N HCl under an N_2 atmosphere. Acid volatile sulfide (as $H_2{}^{35}S$) produced by the reaction was entrained in flowing nitrogen and bubbled into a 10% zinc acetate trap (10 ml) to produce zinc sulfide. The radioactivity of the zinc sulfide (1-ml aliquot) was counted using a Beckman LS 6500 scintillation counter to determine the percentage of added $^{35}SO_4$ that had been converted to [^{35}S]sulfide.

The rate constant (*k*) for DAsR and dissimilatory sulfate reduction (DSR) for each depth interval was derived from the maximum linear rate of radiotracer reduction measured during the incubation time (i.e., the maximum observed percentage of turnover per hour). We calculated estimated in situ rates of DAsR and DSR for each depth interval using the following relationship: rate = $k \times C$, where *k* is the derived rate constant for the depth interval and *C* is the ambient concentration of As(V) or sulfate measured in the sedimentary pore water of that interval. The results for DAsR were expressed based on the total radiotracer activity recovered from each sample following the extraction and ion-exchange speciation procedure, and they did not include small quantities of radiotracer that were retained on the sediments, ion-exchange columns, or syringes (see Results for recovery data). The proportion of $^{73}As(V)$ retained on the ion-exchange columns following As speciation was comparable to the proportion observed for radiolabeled blanks (data not shown).

Searles Lake [^{35}S]sulfate reduction: sediment slurry experiments. An effort was made to more closely monitor sulfate reduction in SL by performing a series of experiments with slurried sediments. In the first experiment, surface sediment was slurried (1:2) with full-strength brine water (salinity, ~346 g/liter) in an electric blender while it was bubbled with N_2 gas. The homogenate (5 ml) was dispensed into 57-ml serum bottles containing an additional 15 ml of either full-strength brine or brine that was diluted with deionized water to 75%, 50%, or 25% of full strength. Triplicate bottles were capped and sealed under N_2, injected with 500 kBq [^{35}S]sulfate, and incubated in the dark at 20°C with constant rotary shaking (100 rpm). After 72 h, the bottles were injected with 2 ml of a 10% zinc acetate solution and stored at −70°C until distillation processing and trapping of [^{35}S]sulfide as described above. In subsequent experiments, an artificial Searles Lake brine was employed, which was composed of NaCl (180 g/liter), Na_2SO_4 (100 g/liter), K_2SO_4 (30 g/liter), $(NH_4)_2SO_4$ (0.05 g/liter), KH_2PO_4 (0.08 g/liter), K_2HPO_4 (0.15 g/liter), $MgSO_4 \cdot 7H_2O$ (0.025 g/liter), Na_2WO_4 (0.075 g/liter), H_3BO_4 (4.0 g/liter), Na_2SeO_4 (0.00001 g/liter), Na_2CO_3 (27 g/liter), $NaHCO_3$ (5 g/liter), and the trace elements solution of Widdell et al. (49) (5 ml/liter). In a second experiment, slurries were prepared as described above except that either full-strength artificial medium (salinity, 346 g/liter) or a highly diluted version of this medium (salinity, 50 g/liter) was used. Homogenate (10 ml) was dispensed into 72-ml serum bottles containing 20 ml of the artificial brines, but the bottles were sealed under an H_2 atmosphere instead of an N_2 atmosphere. Duplicate live slurries were prepared for each brine condition, along with one autoclaved (1 h) control. Slurries were injected with 1,850 kBq of [^{35}S]sulfate and incubated as described above. Subsamples (5 ml) were withdrawn after 24, 48, 120, and 148 h of incubation, and [^{35}S]sulfide was extracted by immediate injection into the distillation vessel as described above. In the final experiment, an attempt was made to lower the overall sulfate content of the materials by washing (see below) in order to increase the specific activity of the added radioisotope. Washing also had the effect of removing As(V), thereby preventing the activity of sulfide-oxidizing, As(V)-respiring chemoautotrophs (8, 29) from removing any [^{35}S]sulfide formed by sulfate reduction. Washing was performed by first adding 40 ml of sediment to a 250-ml centrifuge bottle that contained 100 ml of either high-salinity (340 g/liter), high-sulfate (0.2 M) artificial brine or low-salinity (64 g/liter), low-sulfate (0.02 M) brine and then capping the bottles and stir mixing the contents for 1 h. All manipulations took place in an anaerobic glove bag. The sediment-brine mixtures were then centrifuged, each supernatant was decanted, and the sediment was homogenized with the corresponding artificial brine (1:4) in a blender under N_2. The resulting homogenates (10 ml) were dispensed into 72-ml serum bottles that contained 20 ml of the corresponding artificial brines and were sealed under N_2. All samples received additional electron donor amendments consisting of either 10 mM sodium acetate or 10 mM sodium lactate, or the N_2 atmosphere was replaced with H_2 by 10 min of gas phase flushing. Three live controls (i.e., without added electron donors) and one autoclaved control were prepared for the high-salinity, high-sulfate and low-salinity, low-sulfate conditions and incubated as described above. Subsamples (5 ml) were withdrawn after 0, 168, and 336 h of incubation, injected into Vacutainers containing 1 ml of a 10% zinc acetate solution, and stored at −70°C until the [^{35}S]sulfide content was analyzed as described above.

Total DNA extraction and quantification. Nucleic acid was extracted and purified from 0.5 g (wet weight) of sediment with a FastDNA SPIN kit for soil (Qbiogene, Irvine, CA). All DNA extractions were performed in triplicate, and the extracts were combined to minimize effects from extraction variability and then stored at −80°C until they were assayed. Total DNA concentrations were determined by determining the absorbance at 260 nm with a Nanodrop ND-1000 spectrophotometer (NanoDrop Technologies, Rockland, DE).

DGGE PCR amplification and DGGE analysis. Partial 16S rRNA genes were amplified by using primer 341F (5′-CCTACGGGAGGCAGCAG-3′) with a 40-bp GC clamp (5′-CGCCCGCCGCGCGCGGCGGGCGGGGCGGGGGCA CGGGGGG-3′) and primer 518R (5′-ATTACCGCGGCTGCTGG-3′) (23). PCR amplification was performed using a Peltier PTC-200 thermal cycler (MJ Research Inc., Watertown, MA) and a 50-μl reagent mixture containing approximately 50 ng of template DNA, 10 mM Tris-Cl (pH 8.5), 40 mM KCl, each deoxynucleoside triphosphate at a concentration of 100 μM, 1.5 mM $MgCl_2$, 2 U of *Taq* polymerase, and each primer at a concentration of 0.2 μM. After an initial denaturing step at 94°C for 5 min, the PCR conditions were 30 cycles of denaturation for 30 s at 94°C, annealing for 30 s, and extension for 30 s at 72°C; the initial annealing temperature was 65°C, which was decreased by 0.5°C each cycle for 20 cycles, and this was followed by 10 cycles with an annealing temperature of 55°C. The cycling procedure was followed by final extension at 72°C for 7 min. The PCR product was stored at −80°C prior to DGGE analysis.

DGGE was performed with the D-Code universal mutation detection system (Bio-Rad Laboratories, Inc., Hercules, CA). The gradient gel was cast using a Bio-Rad model 475 gradient delivery system. The denaturing gradients ranged from 40 to 60% denaturant, and 100% denaturant contained 7 M urea and 40% formamide in an 8% (wt/vol) polyacrylamide gel (23). Twenty microliters of PCR product was mixed with 20 μl of 2× loading dye (70% glycerol, 0.05% bromophenol blue, 0.05% xylene cyanol, 2 mM EDTA) and loaded onto the gel. The electrophoresis conditions were 50 V at 60°C for 800 min. A customized DGGE marker with 12 bands at different positions was used as a reference to normalize band positions for comparisons between gels. DGGE gels were stained with ethidium bromide (0.5 μg ml^{-1}), and bands were visualized with a Bio-Rad UV transilluminator. Digital images of the gel were captured with the Quantity-One software (version 4.3.1; Bio-Rad) for use in comparative image analyses. A similarity dendrogram was generated with GelCompar II (version 4.0; Applied Maths, Kortrijk, Belgium) using the unweighted pair group method with arithmetic means based on Dice correlation coefficients.

DGGE band sequencing. Bands selected for identification were excised from the gel with sterile pipette tips (TSP1.5; GelCompany) attached to a band picker (PDM1.5; GelCompany). After freeze-thawing in 20 μl of sterile water to elute the DNA from the gel, 1 μl of eluate was used as a template for PCR amplification with primers 357F (5′-CCTACGGGAGGCAGCAG-3′) and 518R. Amplification was performed as described above, and PCR products were sequenced with the 357F primer. The identity of the nearest neighbor was determined by a BLASTn search of the GenBank database (http://www.ncbi.nlm.nih.gov/BLAST).

16S rRNA gene sequence analysis for the SLAS-3 environmental clone. Nearly full-length 16S rRNA genes were PCR amplified with primers 27F (5′-AGAG

TTTGATCMTGGCTCAG-3′) and 1492R (5′-GGYTACCTTGTTACGACTT-3′) and cloned into the pCR2.1 vector by using a TOPO TA cloning kit (Invitrogen, Carlsbad, CA) as previously described (42). Twenty clones were selected, and the insert DNA was amplified with DGGE primers and run on DGGE gels along with the DGGE PCR product from SL sediment samples as described above. Clones that migrated to the same position as the SLAS-3 DGGE band in the original sample were run on DGGE gels a second time with the SL sample to confirm the band position. Clones whose bands exactly matched the SLAS-3 DGGE band were selected and sequenced. Nearest-neighbor identification and similarity were determined by a BLASTn search of the GenBank database (http://ncbi.nlm.nih.gov/BLAST).

Consensus *arrA* primer design. The *arrA* genes from *Shewanella* sp. strain ANA-3, *Desulfitobacterium hafniense*, *Sulfurospirillum barnesii* SES-3, strain MLMS-1, *Bacillus selenitireducens*, *Bacillus arseniciselenatis*, and *Chrysiogenes arsenatis* were aligned using ClustalX. *arr*A consensus primers were designed from the multiple-sequence alignment using the program CODEHOP (http://blocks.fhcrc.org/codehop.html). The archaeal codon bias of *Halobacterium* was used in the initial parameters of CODEHOP. Nineteen primers targeting various conserved amino acid blocks in the ArrA multiple sequence alignment were selected and tested in PCRs with various forward and reverse primer combinations. The final primer set, primers HAArrA-D1F (5′-CCGCTACTACACCGA GGGCWWYTGGGRNTA-3′) and HAArrA-G2R (5′-CGTGCGGTCCTTGA GCTCNWDRTTCCACC-3′), produced a 500-bp PCR product.

PCR amplification of *arrA* genes. Each 30-μl PCR mixture consisted of 10 mM Tris-Cl (pH 8.5), 50 mM KCl, 2.5 mM $MgCl_2$, each deoxynucleoside triphosphate at a concentration of 100 μM, each primer at a concentration of 0.33 μM, 1 U of *Taq* polymerase, and approximately 20 ng of DNA. The PCR conditions used were initial denaturation at 95°C for 5 min, followed by 40 cycles of denaturation at 94°C for 30 s, primer annealing at 53.5°C for 30 s, and extension at 72°C for 30 s, with an additional step at 85°C for 10 s. Five microliters of PCR product was visualized by UV fluorescence following electrophoresis in a 1.5% agarose gel in SB buffer at 150 V for 30 min by staining with a 100-μg ml^{-1} ethidium bromide solution for 10 min and destaining with deionized water for 5 min.

Cloning and sequencing *arrA* genes. The PCR products were purified using a QIAGEN PCR cleanup kit according the instructions of the manufacturer. Clone libraries were constructed using a TA TOPO plasmid cloning kit from Invitrogen. Approximately 50 clones of the PCR product were screened for the correct plasmid insert size by PCR using the M13 vector primers. DNA inserts from the plasmids were sequenced using the M13F primer.

Nucleotide sequence accession numbers. The DNA sequences are available in the GenBank database under accession no. DQ858358 to DQ858445 for *arrA* sequences and DQ849091 to DQ849117 for 16S rRNA gene sequences.

RESULTS

Sediment arsenate and sulfate reduction radiotracer experiments. Incubated sediments from all depths of both lakes showed progressive reduction of $^{73}As(V)$ to the reduced products $^{73}As(III)$ and [^{73}As]thioarsenite. The results for the most active samples for each lake (0- to 2-cm depth for ML; 2- to 4-cm depth for SL) are shown in Fig. 1. In both cores, the reduction of $^{73}As(V)$ was accompanied by corresponding increases in the levels of aqueous $^{73}As(III)$ as well as [^{73}As]thioarsenite reduction products. Most of the $^{73}As(V)$ reduced in the upper 2 cm of ML sediments was recovered as [^{73}As]thioarsenites, which accounted for 49% of the added counts, compared to the 18% of counts recovered as aqueous $^{73}As(III)$. In contrast, the majority of $^{73}As(III)$ recovered in the SL sediments was present as the aqueous form (26% of the added counts), and [^{73}As]thioarsenites represented only 4% of the added counts. This difference in [^{73}As]thioarsenite products can be explained by the greater abundance of sulfide in sediments from ML than in sediments from SL (see below).

The progress curves for all the depths examined are shown in Fig. 2A for ML and in Fig. 2B for SL. Collectively, the average levels of recovery of added ^{73}As with this method for all the depths sampled were 86% (standard deviation, 6%; n = 48) for ML sediments and 88% (standard deviation, 11%; n = 48) for SL sediments. On average, approximately 6% of the radiotracer activity added remained associated with the sediment plugs from both lakes following the phosphate extraction procedure. The remaining minor quantities of unrecovered ^{73}As were retained on the ion-exchange columns or as residual material on the syringes and centrifuge tubes used during the extraction and speciation process. DAsR activity was entirely abolished by autoclaving sediment slurries (ML) or subcores (SL) (data not shown). As noted above, the highest rates of $^{73}As(V)$ reduction occurred near the top of the core profile in ML (Fig. 2A) and SL (Fig. 2B). The derived rate constants for DAsR activity in ML decreased steadily with depth and ranged from 0.103 h^{-1} at the top (0 to 2 cm) to 0.004 h^{-1} at the bottom (18 to 22 cm). The corresponding rate constants for SL were 0.006 h^{-1} at the top and 0.002 h^{-1} at the bottom, with the maximum value (0.012 h^{-1}) observed at 2 to 4 cm.

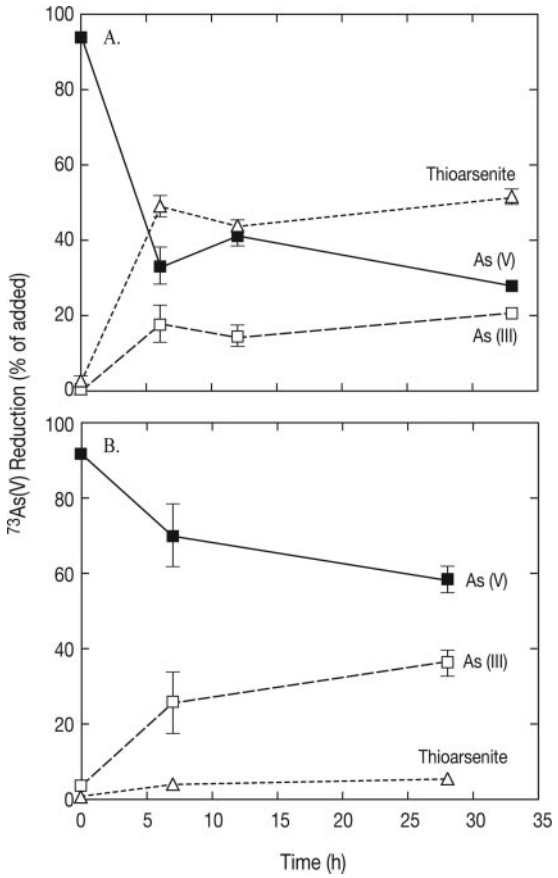

FIG. 1. Time course of $^{73}As(V)$ incubation of sediments from Mono Lake (A) and Searles Lake (B). The symbols indicate averages for two samples, and the error bars indicate the ranges of values.

Sulfate reduction was detected at all depths sampled in the ML core, and the production of [^{35}S]sulfide was linear for all these depths during the 33-h assay (data not shown). The samples with the highest [^{35}S]sulfate reduction activity corresponded to those with $^{73}As(V)$ reduction activity and were from the upper 0 to 2 cm of the sediment (k = 0.00076 h^{-1}). These surficial sediments accounted for 93% of the total [^{35}S]sulfide produced at all the depth intervals sampled in the

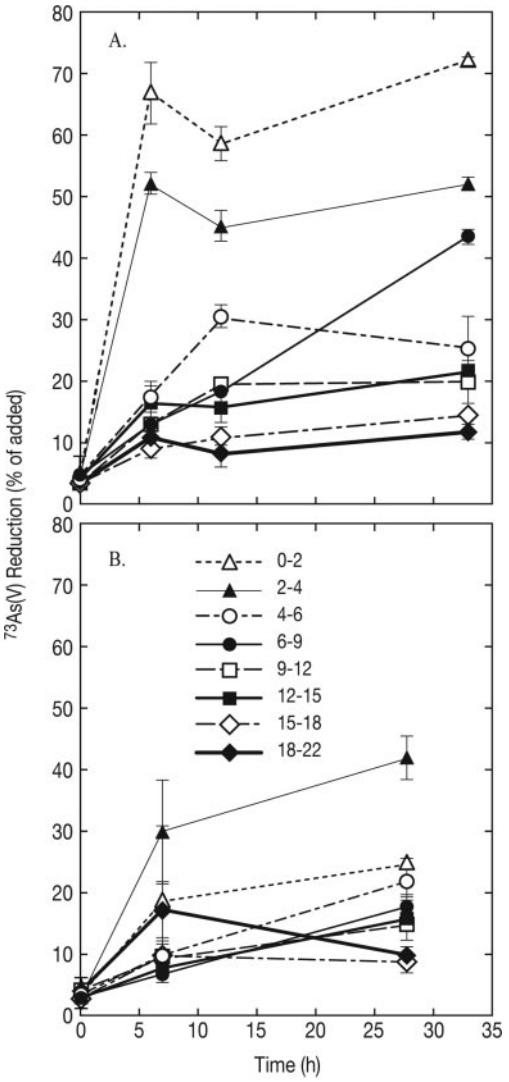

FIG. 2. ^{73}As(V) reduction activity in subcores from different depths (in centimeters) in Mono Lake (A) and Searles Lake (B) sediment cores. The symbols indicate averages for two samples, and the error bars indicate the ranges of values.

ML core. The rate constants for sulfate reduction at depths below 4 cm varied between 0.000006 and 0.000009 h^{-1}. In stark contrast to these results, however, no [^{35}S]sulfide production was detected in any of the sediment subsamples taken from any of the depths assayed in the SL core over the time course of the radioassay incubation (detection limit, 0.2 nmol ml^{-1} h^{-1}) (data not shown).

Incubation of Searles Lake sediment slurries also failed to demonstrate production of [^{35}S]sulfide from [^{35}S]sulfate added to live samples under a variety of experimental conditions meant to promote the activity of sulfate reducers (data not shown). In the first experiment, conducted with natural brine and dilutions of this brine, no activity was detected after 72 h of incubation. In the second experiment, conducted with artificial brines with either high or low salinity, no activity was detected in live samples incubated in the presence of H_2 during the 148 h of incubation. In the third experiment, where washing was employed to lower the sulfate content of the sediments and thereby increase the final specific activity of the [^{35}S]sulfate added, no activity was discerned at any time during prolonged incubation (336 h) in any of the high- or low-salinity samples, even the samples that were amended with the substrate H_2, lactate, or acetate. In all cases, the trapped counts for the live samples were statistically identical to those for the autoclaved controls, which were statistically identical to the counts for blank samples (~40 cpm).

Sediment pore water profiles of chemical constituents and DAsR and DSR activities. The ML concentration profiles, as well as the rates of DAsR and DSR, are shown in Fig. 3. The concentrations of dissolved methane, phosphate, and ammonia all increased with depth, reaching maximum values of 0.8, 2.1, and 3.0 mM, respectively, near the bottom of the core (Fig. 3A). The dissolved chloride content decreased slightly with depth from 0.5 molality (*m*) in the overlying water to 0.4 *m* at the base of the core. The oxidation state of As changed from ~200 μM As(V) in the overlying water to entirely As(III) (as arsenite plus thioarsenite) in the sediment by the first depth interval (2 cm) sampled (Fig. 3B). Thioarsenites were the dominant As species at most depths in the ML sediment profile. The pore water thioarsenite concentration in ML ranged from 75 to 156 μM, representing 43 to 71% of the total measured As(III). These results are consistent with those of Hollibaugh et al. (9), who reported that thioarsenites were the dominant portion of arsenic in the +3 oxidation state occurring in the anoxic bottom waters of ML. In situ rates of As(V) reduction could not be calculated for the ML sediments because of the absence of detectable pools of As(V) at the depth intervals sampled. The highest rates of ^{73}As(V) turnover, accounting for 74% of the observed activity, were confined to the upper 4 cm of sediment and are shown in Fig. 3B as the rate constants rather than the actual rates. Therefore, it seems likely that the in situ DAsR activity occurred on a finer vertical scale than was sampled during this study (e.g., 0 to 0.2 cm versus 0 to 2.0 cm).

Sulfate concentrations decreased linearly from >105 mM in the overlying water column and the uppermost core sections to 62.1 mM at the base of the core (Fig. 3C). The loss of sulfate was accompanied by an increase in the sulfide concentration with depth. The highest rate of sulfate reduction in the ML core (53.4 nmol ml^{-1} h^{-1}) was found in the 0- to 2-cm depth interval. Considerably lower rates of sulfate reduction activity were measured deeper in the ML core (average rate for depths below 2 cm, 0.6 nmol ml^{-1} h^{-1}).

The pore water chemical and activity profiles for SL are shown in Fig. 4. The dense brine immediately underlying the salt crust was diluted by the influx of freshwater caused by penetration of the salt crust. This sampling artifact was evident in the much lower chloride and phosphate concentrations found in the overlying brine than in the underlying pore water samples (Fig. 4A). The methane and ammonia concentrations increased with sediment depth, although the values at 20 cm were three- and fivefold lower, respectively, than those at the same depth in ML (Fig. 3A). On the other hand, the interstitial phosphate levels were nearly 1 order of magnitude higher in SL, and the chloride concentration remained constant with depth. The sulfide concentrations were about 50-fold lower in SL (Fig. 4C) than in ML (Fig. 3C). Our previous pore water data for SL were obtained from a core processed on-site (29)

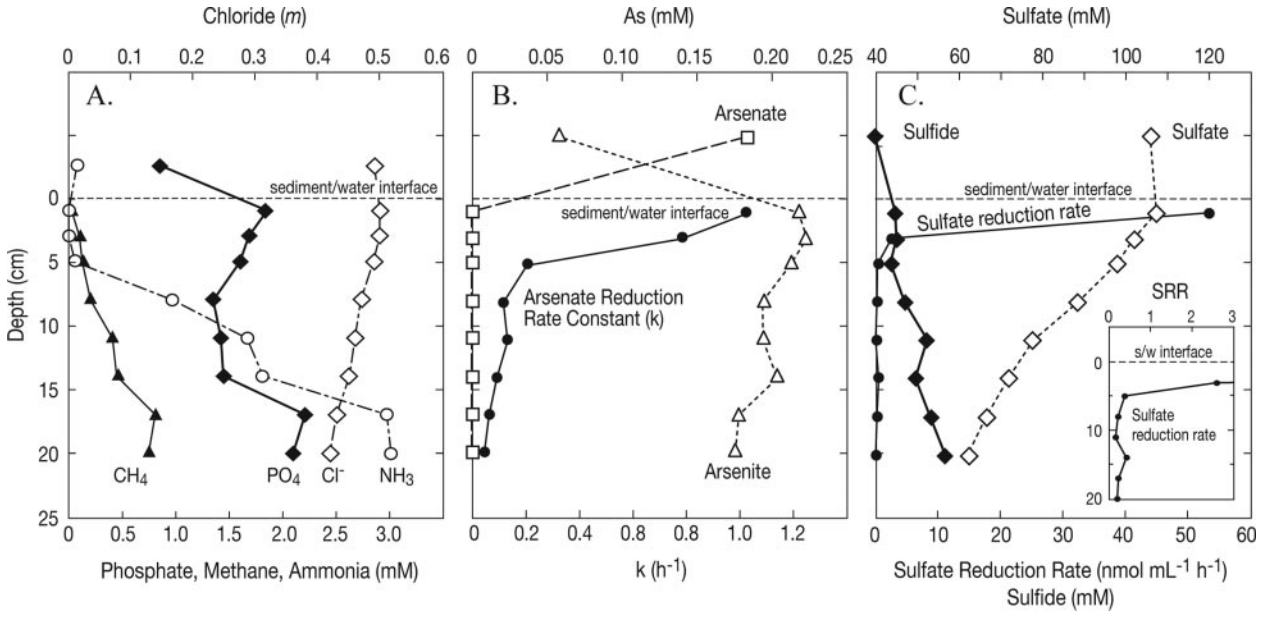

FIG. 3. Mono Lake core profiles for dissolved constituents (A), arsenic speciation and arsenate reductase activity expressed as the rate constant (B), and sulfate, sulfide, and sulfate reductase activities (C). The actual arsenate reduction rate was zero at the sediment depths sampled, which reflects the lack of a detectable ambient arsenate pool rather than a lack of activity. The inset in panel C shows the sulfate reduction rates (SRR) detected at different depths using a finer scale. s/w interface, sediment-water interface.

that gave concentration ranges for methane (0.025 to 0.51 mM), ammonia (0.34 to 1.2 mM), and sulfide (0.06 to 0.17 mM) that were roughly comparable to our current data. This indicates that the transportation of the core back to our laboratory in Menlo Park, CA, did not result in significant increases in or losses of these constituents, and hence our comparisons of the pore water concentrations to those of ML are valid.

The brine dilution that occurred during sampling also accounted for the lower concentrations of As(V) (~0.9 mM) (Fig. 4B) and sulfate (~80 mM) (Fig. 4C) in the overlying brine compared to measurements that we obtained previously (29) when there was no such dilution after sampling [As(V) concentration, 3.9 mM; SO_4^{2-} content, ~0.7 *m*]. Arsenic was present entirely as As(V) in the overlying brine, but As(III)

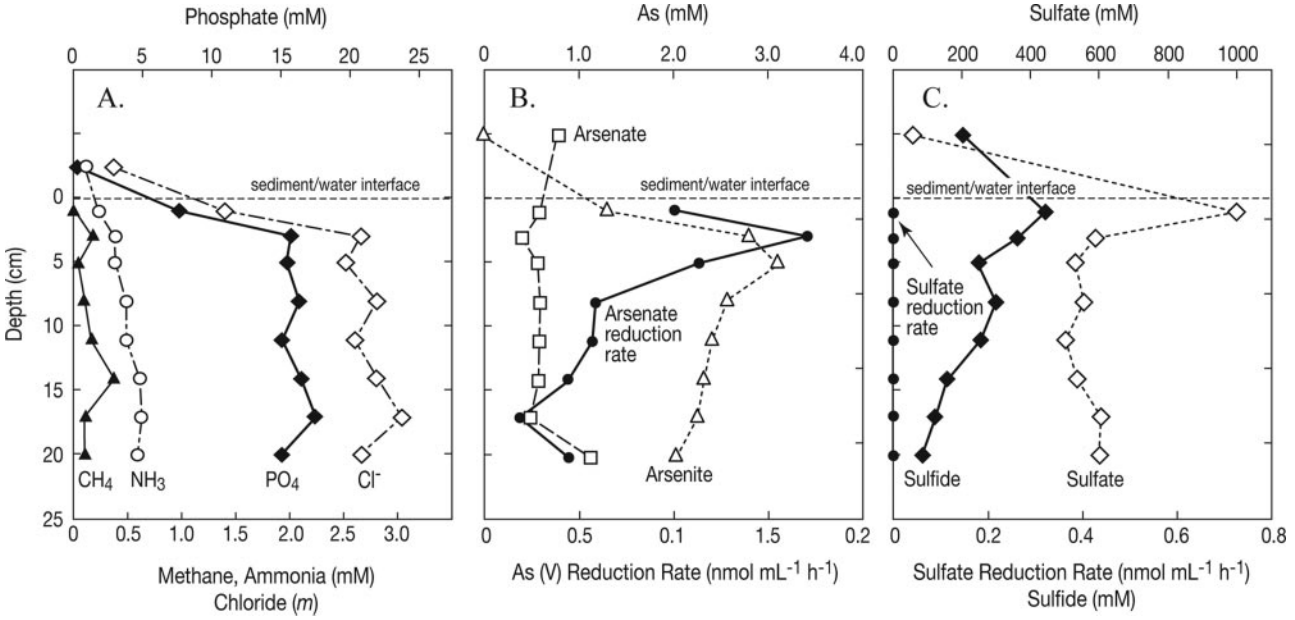

FIG. 4. Searles Lake core profiles for dissolved constituents (A), arsenic speciation and arsenate reductase activity (B), and sulfate, sulfide, and sulfate reductase activities (C). The concentrations of the constituents above the sediment-water interface were reduced due to dilution by rainwater runoff during sampling.

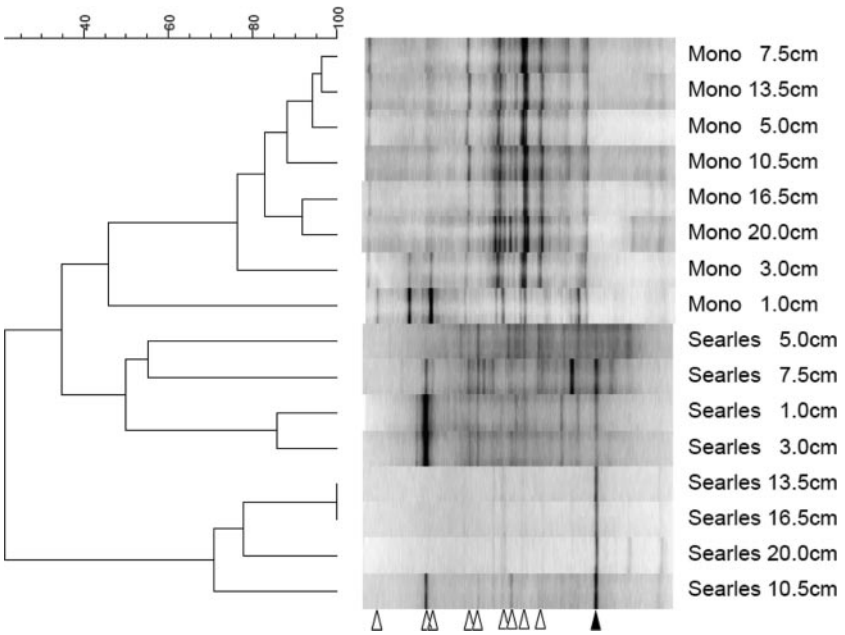

FIG. 5. DGGE of 16S rRNA of SL and ML sediment cores. The similarities between samples are shown in a unweighted pair group method with arithmetic mean dendrogram of Dice similarity coefficients, a parameter that takes only band position and not band intensity into account; the scale bar indicates levels of similarity. The open arrowheads indicate bands that were related to cyanobacteria; the solid arrowhead indicates the band related to chemoautotrophic arsenate-respiring isolate SLAS-1.

immediately became the predominant oxidation state with the transition into the sediment environment (Fig. 4B). In contrast to ML pore water, aqueous As(III) was the predominant form of reduced As in SL pore water. Thioarsenite concentrations similar to those observed in ML were obtained for several depth intervals of the SL core (maximum concentration, 230 μM). Nonetheless, thioarsenites represented less than 10% of the total amount of As(III) in SL pore water owing to the relatively high arsenite and low sulfide concentrations at all sediment depths compared to the concentrations in ML. The SL sediments were characterized by a relatively uniform pool of dissolved As(V) (average concentration, 0.6 mM) at all depths in the sediment core. The presence of an ambient As(V) pool with depth in the core allowed calculation of DAsR rates based on the measured rate of radiotracer reduction. The highest rate of As(V) reduction (1.72 nmol ml^{-1} h^{-1}) was obtained for the 2- to 4-cm depth interval, and the majority (63%) of the DAsR activity observed occurred in the upper 6 cm of sediment (Fig. 4B). Arsenate reduction occurred at significant rates at all depth intervals of the core, and the average rate for depths below 6 cm was 0.45 nmol ml^{-1} h^{-1}.

The SL pore water contained very high concentrations of dissolved sulfate, which decreased abruptly from ~1,000 mM in the 0- to 2-cm depth interval to 589 mM in the 2- to 4-cm interval (Fig. 4C). Below 4 cm, however, the concentration of dissolved sulfate was fairly uniform (~560 mM) throughout the remaining depth of the core. The rapid decrease in the sulfate concentration observed in the upper 4 cm of this core was not accompanied by a corresponding increase in the concentration of dissolved sulfide. Indeed, the sulfide concentration generally decreased steadily with depth. This vertical profile of dissolved sulfate and sulfide concentrations suggests an absence (or near absence) of active DSR activity in the sediments, and this interpretation is supported by the complete lack of [^{35}S]sulfide production in sediment from any depth interval of the SL core during the radioassay incubation.

DGGE analysis of 16S rRNA genes of the microbial populations. DGGE analysis of 16S rRNA genes amplified from ML and SL sediment samples showed that the ML and SL sediment microbial communities were distinct from each other (Fig. 5). The ML sediment microbial community was quite similar throughout the sediment core with the exception of the surface sample (depth, 0 to 2 cm), which was distinct from the samples from the other depths. SL sediment microbial communities were less well conserved with depth. At least three separate groups were seen: surface samples (0 to 4 cm), mid-depth samples (5 to 9 cm), and bottom samples (10 to 20 cm). These observations are consistent with the observed dramatic color shift from black to greenish at 10 cm in the sediments (data not shown).

Sequence analysis of selected DGGE bands indicated the presence of a diverse community of cyanobacteria in the upper 0 to 4 cm of sediments from both ML and SL sediments (Fig. 5). Several of these bands were also present in deeper sections of both cores. One band that was prominent in SL sediments from depths below 3 cm but was absent from the ML sediments was closely related to strain SLAS-1, an extremophilic As(V) respirer recently isolated from these sediments (29). An approximately 900-bp clone matching this band was most similar to gene sequences retrieved from the alkaline, hypersaline lakes of the Wadi An Natrun, Egypt (98% similarity; unpublished GenBank submission by N. M. Mesbah, S. H. Abou-El-Ela, and J. Wiegel; accession number DQ432325), which also

exhibited 95% similarity with SLAS-1; this clone has been designated SLAS-3.

***arrA* gene analysis of the microbial populations.** The consensus *arrA* primers developed by Malasarn et al. (18) were initially used to detect *arrA* in DNA extracts from ML and SL sediments. However these primers yielded weak PCR products only for the upper layer of the sediment cores. A new primer set was constructed using the same methods employed by Malasarn et al.; however, the amino acid codon bias for *Halobacterium*, a halophilic archaeon, was used in the final DNA sequences in the conserved core region of the new primers (designated HAarrA). PCR products were detected in all but the deepest sample of the ML sediments using the HAarrA primer set; however, these PCR products were detectable only in the upper ~10 cm of the SL sediment (Fig. 6). Although PCR amplification is subject to many biases and thus is not quantitative, the trend based upon the amount of PCR product appeared to be a decrease in *arrA* concentration with depth in both sediments.

The diversity of the 500-bp HAarrA-amplified gene fragments was determined by constructing several clone libraries and sequencing ~50 clones per library. BLAST searches of the translated DNA sequences showed that they were most similar to the DNA sequence for arsenate respiratory reductase, ArrA. The levels of amino acid sequence similarity ranged from 70% to 80% for comparisons with various ArrAs of known arsenate-respiring prokaryotes, such as *B. arseniciselenatis*, *B. selenitireducens*, and *Shewanella* sp. strain ANA-3. Many of the ML and SL sequences were also similar (~70 to 80% amino acid sequence similarity) to an *arrA*-like sequence identified in the recently completed genome sequence of the metal-reducing alkaliphilic bacterium *Alkaliphilus metalliredigenes* (52). It is not know whether this bacterium respires arsenate; however, it was isolated from an alkaline leachate pond containing high arsenic concentrations (1.7 mM). A phylogenetic reconstruction based on the translated ML and SL sequences is shown in Fig. 7. Most of the sequences were very similar, differing by only 4 to 10 amino acids. Many of the SL and ML clones were nearly identical. However, there were three SL clusters and one ML cluster that had the most unusual ArrA sequences. SL cluster II comprised four SL clones that were most similar (82 to 85% amino acid similarity) to an *arrA*-like sequence in the MLMS-1 genome sequence (NCBI accession no. EAT04932).

To determine if any of the ArrA sequences from the SL sediments matched that of SLAS-1, the arsenate respirer previously isolated from these sediments, we determined the sequence of the ArrA gene from SLAS-1. The new HAarrA primers did not produce a product with SLAS-1 DNA; however, the primers of Malasarn et al. (18) produced a PCR fragment that was the correct size. After the sequence of this product was obtained, phylogenetic analysis showed that the SLAS-1 sequence was an ArrA homolog that was most similar to the ArrA of *S. barnesii* and *C. arsenatis* and was not closely related to any sequences obtained directly from the sediments (Fig. 7). This placement of SLAS-1 is tentative due to the limited sequence data used in the phylogenetic analysis (~40 amino acid residues).

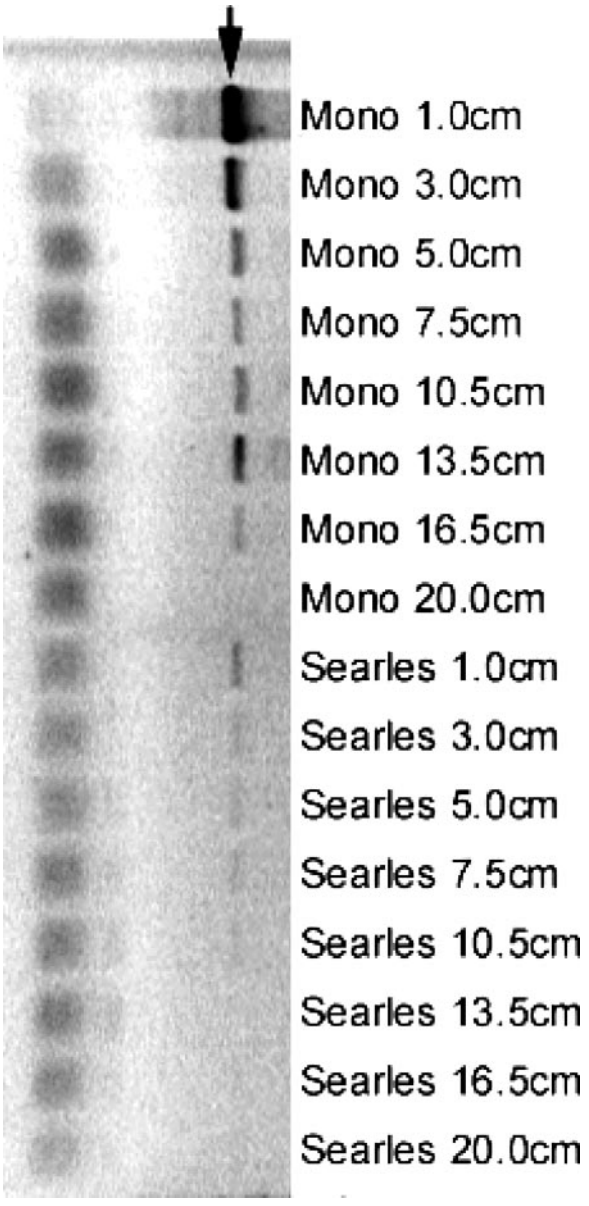

FIG. 6. *arrA* PCR products from SL and ML sediment cores. The arrow indicates the expected position (~550 bp) of the *arrA* PCR product.

DISCUSSION

Sediments from all depths of both the ML and SL cores sampled exhibited As(V) reductase activity (Fig. 2). However, sulfate reduction was observed only in the ML sediments and was not detected in any of the SL sediment samples. The absence of sulfate reduction in SL sediments can be attributed to the bioenergetic constraints imposed on certain anaerobic prokaryotes by the salt-saturated conditions prevalent in SL. Oren (35) proposed that the oxidation of electron donors (e.g., hydrogen) with sulfate, or with CO_2 in the case of methanogens, does not supply sufficient metabolic energy to allow anaerobes to physiologically maintain an internal salt concentration that is much lower than that of their saturated external

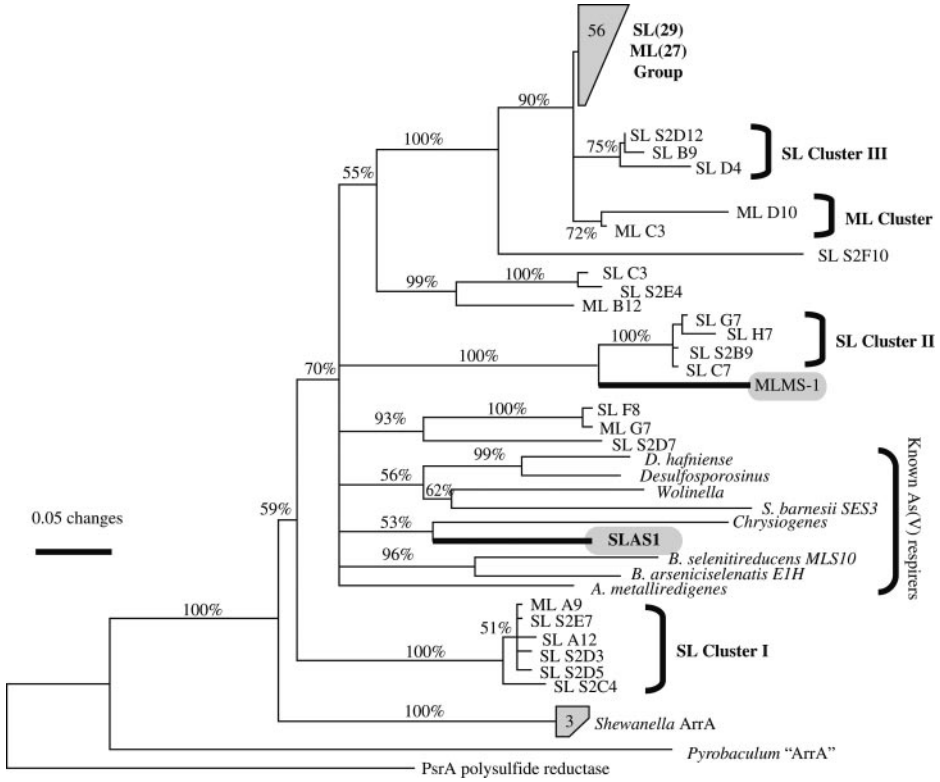

FIG. 7. Phylogenetic relationships based on partial ArrA sequences from Mono Lake and Searles Lake sediments. SL and ML indicate sequences originating from Searles Lake and Mono Lake sediments, respectively (accession no. DQ858358 to DQ858445). The partial ArrA sequences of the clone libraries were aligned with various known sequences using ClustalX. The tree was constructed by neighbor-joining analysis of the distance matrix generated by DNADIST in Phylip with a Kimura two-parameter transition-transversion model. Bootstrap values of at least 50% for 1,000 replicates are indicated at the nodes. The scale bar indicates 0.05 change per site. The following organisms are included: *B. selenitireducens* strain MLS10 (accession no. AY283639), *B. arseniciselenatis* strain E1H (AY660885), *C. arsenatis* (AAU11839), *Desulfosporosinus* sp. strain Y5 (DQ220794), *Shewanella* sp. strain ANA-3 (AAQ01672), *Shewanella* sp. strain W3-18-1 (ZP_00904618), *Wolinella succinogenes* DSM 1740 (NP_906980), MLMS-1 (EAT04932), *A. metalliredigenes* strain QYMF (ZP_00800578), *S. barnesii* strain SES-3 (AAU11840), and *P. aerophilum* (AAL64489).

milieu (>240 g/liter). Arsenate, however, is a more thermodynamically favorable bio-oxidant than sulfate (for $HAsO_4^{2-}$/$H_2AsO_3^-$, $E_0' = 60$ mV; for SO_4^{2-}/HSO_3^-, $E_0' = -516$ mV) and thus is a more robust electron acceptor (27, 29). This explains why dissimilatory As(V) reduction was operative in the sediments from both lakes, while sulfate reduction could be detected only in the moderately hypersaline ML.

An alternative explanation, however, is simply that the higher-potential oxyanion As(V) must be entirely depleted from the pore water before the lower-potential oxidant sulfate can be consumed. Such a sequential phenomenon of oxidant usage has long been observed with depth in sediments, where consumption of stronger oxidants like nitrate, Mn(IV), and Fe(III) sequentially precedes removal of sulfate and methanogenesis occurs last. The experimental record with sulfate reducers capable of dissimilatory As(V) reduction, however, is mixed. Newman et al. (24) reported that As(V) reduction preceded reduction of sulfate during growth of *Desulfotomaculum auripigmentum*, while Macy et al. (17) reported simultaneous reduction of both sulfate and As(V) by *Desulfomicrobium* sp. strain Ben-Rb.

Despite our inability to detect [^{35}S]sulfate reduction in SL, about 0.2 mM sulfide and a similar concentration of methane were present at depth in pore waters of the sediments (Fig. 4). Presumably, these concentrations each resulted from ongoing microbial processes. These concentrations were roughly 75-fold less and 4-fold less, respectively, than the concentrations observed in ML at comparable depths (Fig. 3). Hence, extreme salinity does appear to have had a considerable dampening effect on the expression of these two low-energy-yielding anaerobic microbial processes in SL compared with ML. This suggests that the hypothesis of Oren (35) is essentially valid but that there are substantial decreases in these processes at salt saturation rather than a complete shutdown (20). In addition, radiotracer studies of sulfate reduction in salt-saturated brines that have abundant sulfate as well as arsenate (Table 1) are a considerable technical challenge. First, there is high isotope dilution of the added [^{35}S]sulfate, and second, any [^{35}S]sulfide produced can be recycled to [^{35}S]sulfate by As(V)-respiring chemoautotrophs having biochemical pathways comparable to those of strains MLMS-1 and SLAS-1 (8, 29). It is therefore quite possible that SL sediments sustained a very low rate of sulfate reduction that simply could not be detected by our radiotracer methodology.

We calculated integrated rates of arsenate and sulfate reduction in the sediments of both lakes based on the reduction

TABLE 2. Rates of dissimilatory arsenate and sulfate reduction measured with radiotracers, compared with arsenate and sulfate concentration gradients, diffusivities, and calculated fluxes from the overlying water to the sediment pore water (depth, 1 cm)

Factor	Reduction rate (mmol m^{-2} day^{-1})	$\delta C/\delta Z$ (μmol cm^{-4})	D_s (cm^2 s^{-1})[a]	Flux (mmol m^{-2} day^{-1})
Mono Lake arsenate	0.30[b]	0.18	3.88×10^{-6}	0.4
Searles Lake arsenate	3.40	2.58[c]	6.06×10^{-7}[c]	0.5[c]
Mono Lake sulfate	27.8	2.70[d]	4.57×10^{-6}[d]	6.7[d]
Searles Lake sulfate	0.00	42.93[c]	7.11×10^{-7}[c]	5.1[c]

[a] D_s, molecular diffusion coefficient at 20°C corrected for viscosity and tortuosity.
[b] Maximum rate based on the detection limit for As(V) (8.3 μM), the radiotracer rate constant in the 0- to 2-cm interval (0.103 h^{-1}), and the As(V) concentration in the overlying water (182 μM).
[c] Calculated using arsenate and sulfate concentrations in undiluted lake water and sedimentary pore water measured during the April 2004 field season.
[d] Values for sulfate diffusion between first and second core depth intervals.

rates observed in the radiotracer experiments (Table 2). Because of the high salt concentrations in the sedimentary pore waters, significant dilution of the samples was required prior to high-performance liquid chromatography–hydride generation atomic absorption spectroscopy analysis. Thus, the functional detection limit for As(V) in these samples was 8.3 μM. Based on this detection limit and the As(V) concentration of the overlying ML water (182 μM), we calculated a maximum penetration depth of 1.8 mm for As(V) in the ML sediment. An integrated As(V) reduction rate of 0.3 mmol m^{-2} day^{-1} in ML sediment was calculated based on this depth using the rate of radiotracer turnover in the upper 2 cm of the core ($k = 0.103$ h^{-1}). By comparison, the Searles Lake integrated As(V) reduction rates were 11-fold higher than those of ML (3.4 mmol m^{-2} day^{-1}). The integrated rate of sulfate reduction in the ML sediments was 27.8 mmol m^{-2} day^{-1}. Sulfate reduction was clearly the dominant anaerobic pathway for respiration and organic carbon mineralization in ML sediments and was greater than arsenate reduction by a factor of 90 on a molar basis and by a factor of 360 on an electron equivalent basis. This sulfate reduction rate was in close agreement with that obtained in a previous study (30) of sulfate reduction in the same sediments (e.g., 28 versus 32 mmol m^{-2} day^{-1}).

Calculated rates of diffusion of arsenate and sulfate into the sediments of both lakes are also shown in Table 2. Calculation of realistic fluxes for SL was not possible with data from the core utilized in the radiotracer experiments (i.e., the core collected in February 2005). This was due to sampling-related dilution of the overlying brine in the SL core (see above), as well as the anomalously high sulfate concentration in the 0- to 2-cm depth interval of this core (Fig. 4). The abrupt decrease in sulfate concentration below 2 cm in this core is perplexing given the absence of detectable sulfate reduction activity in our radioassay experiments and the lack of a corresponding increase in pore water sulfide concentration. Dissolution of solid-phase sulfate minerals from the surficial sediment layer or the overlying salt crust is a possible explanation. An elevated pore water sulfate concentration in the surficial sediment was not observed in a core that we collected and analyzed during a previous, drier field season (April 2004) (29). The range of pore water sulfate concentrations at all depths of the April 2004 core was in close agreement with that observed for depths below 2 cm in the February 2005 core. For these reasons, we calculated diffusive fluxes for SL based on overlying brine and pore water concentrations of As(V) and sulfate that were measured for the April 2004 core.

The calculated rates of downward As(V) diffusion were similar for the two lakes, despite the much steeper concentration gradient between overlying and pore waters in SL than in ML. This was because SL had lower sediment porosity and higher water viscosity. The maximum integrated rate of sedimentary arsenate reduction estimated for ML was roughly equal to the diffusive flux of As(V) into the sediment, while the rate of As(V) reduction in the SL sediment was sevenfold higher than the diffusion into the sediment. These observations indicate that diffusion does not transport sufficient As(V) into the sedimentary pore water of these lakes to exceed consumptive demand. While this explains the absence of As(V) from the ML pore waters (Fig. 3B), it does not reconcile the observation of a residual ~0.6 mM As(V) in the SL sediment (Fig. 4B). Therefore, either our As(V) reduction rates were overestimated or there is an alternate chemical, biological, or physical process that resupplies As(V) to the pore water. Alternately, the dissolution of As(V)-bearing secondary minerals, such as scorodite ($FeAsO_4 \cdot 2H_2O$) or precipitated As(V) salts (e.g., Na_2AsO_4), from the solid sediment phase may contribute to the persistence of As(V) in the pore waters. It is noteworthy that other workers have reported similar disparities, for example, in attempts to reconcile radiotracer-based sulfate reduction rates with residual pools of sulfate in sediments from the Gulf of Mexico (12).

The pore water sulfate concentration of the surficial (0 to 2 cm) sediment layer slightly exceeded the overlying lake water concentration in ML. This indicates that there was net diffusion of sulfate out of the sediment and into the overlying water column, which was possibly a result of sulfide oxidation at the sediment-water interface. In order to estimate the magnitude of diffusion as a source of sulfate in the deeper ML sediments, we calculated rates of downward sulfate diffusion from the first depth interval (0 to 2 cm) to the second depth interval (2 to 4 cm) of the core (Table 2). The total integrated rate of sulfate reduction (27.8 mmol m^{-2} day^{-1}) in ML was significantly higher than the calculated diffusive flux between the first and second depth intervals (6.7 mmol m^{-2} day^{-1}); however, most sulfate reduction activity (25.6 mmol m^{-2} day^{-1}) occurred in the first sediment interval. The integrated rate of sulfate reduction for all sample depth intervals below 2 cm (2.2 mmol m^{-2} day^{-1}) was three times lower than the downward diffusive flux from the first depth interval. This indicates that diffusion may be an important mechanism of sulfate supply to the ML sediment column below 2 cm; however, diffusion alone is not adequate to satisfy the consumptive demand stemming from

sulfate reduction in the near-surface sediments, where biological sulfide oxidation may predominate. The diffusive flux for sulfate into the SL sediment is constrained at 5.1 mmol m^{-2} day^{-1} (based on data from the April 2004 field season); however, the absence of detectable sulfate reduction limits the availability of this sediment as a sink for dissolved sulfate.

The apparent microbial diversity in the lake sediments is low relative to that in marine or freshwater sediments, probably due to the extreme chemical conditions in the lake sediments. This contention is supported by the observation that the apparent diversity is lower in the more extreme lake, SL, than in ML (Fig. 5). Surprisingly, most of the bands sequenced from the upper portion of the sediments in both lakes were related to cyanobacteria, and many of these bands were found throughout the sediments. These bands were even found in the deeper portions of the core well below the point where light can reasonably be expected to penetrate. Sequencing of several of these bands confirmed their relationship to cyanobacteria. This likely indicates the presence of DNA from the sediment surface that was preserved in deeper sediments due to the hypersaline conditions. However, not all DGGE bands were found throughout the sediments: for example, SLAS-3 was found only in the deeper parts of the sediment (Fig. 5). Together, these data imply that the DNA extracted from ML and SL sediments were a mixture of preserved DNA from biologically active and inactive organisms. If these organisms can be distinguished from each other (for example, by examination of RNA to identify the active organisms), the preserved DNA may be an indicator of the history of the surface sediments of the lakes (7).

No bands related to the sulfate-reducing bacteria (SRB) were observed in sediment samples from either lake, despite the high sulfate reduction activity observed in ML. Most dominant bands on the DGGE gel image were sequenced (a total of 13 bands, 4 bands from ML); however, the lack of SRB sequences in the ML sample could well have been the result of undersampling, and one of the unsequenced bands may have been related to SRB.

The sequence designated SLAS-3 was found in SL but not in ML, perhaps indicating a specific affiliation between this gene sequence and the more extreme conditions found in SL. This contention is supported by the high level of similarity (>98%) between this gene sequence and the unpublished sequences recently deposited by Mesbah et al. in the GenBank database from the alkaline, hypersaline lakes of the Wadi An Natrun, Egypt (data not shown). However, whether the relationship with higher salinity is due to a role in DAsR has not been determined yet. Despite the similarity of SLAS-3 to SLAS-1, an extremophilic DAsR isolate from SL sediments (29), the distribution of SLAS-3 in the sediments argues that this organism's role in DAsR in SL sediments is limited. SLAS-3 is prevalent in deeper SL sediments, well below the 2- to 4-cm depth, where the highest As(V) reduction occurred (Fig. 2B), and in a region where *arrA* was nearly or completely undetectable by PCR (Fig. 6). However, DAsR activity was found throughout the sediment core; thus, a different organism or group of organisms may be involved in DAsR in the surficial sediments, while SLAS-3 may be more involved in deeper sediments.

While it is a quantitative measure of neither the actual abundance of *arrA* nor its expression, the concentration of the *arrA* PCR product in the total DNA extracts correlated with the observed DAsR activity in sediments from both lakes; however, more *arrA* PCR product was detected in ML sediments than in SL sediments despite a calculated integrated DAsR activity that was 11-fold higher in SL sediments (Fig. 6). Furthermore, the lack of detectable *arrA* gene product in the deeper core sections is intriguing, as DAsR activity was found in all samples. These discrepancies indicate either increased efficiency of a particular ArrA enzyme in SL so that undetectable gene concentrations are still sufficient for greater activity, greater expression of low-abundance *arrA* genes, PCR biases, or the presence of novel dissimilatory arsenate reduction genes. It is impossible to distinguish between these possibilities at this time. Examining the RNA fractions to determine *arrA* abundance and diversity would help unravel these issues.

The diversity of *arrA* suggests that there are unique ArrA phylotypes (e.g., SL clusters I, II, and III) found only in SL and that there are several distinct sequences in ML (ML cluster). Most *arrA* sequences were found in both ML and SL sediments, suggesting either that there was transmission by horizontal gene transfer or that these sequences represent an unidentified population(s) of arsenate-respiring prokaryotes. In comparison, the sequences retrieved in this study are different from the sequences retrieved by Hollibaugh et al. (10) using the primers of Malasarn et al. (18) with ML water column samples. On average, the SL, ML, and SLAS-1 sequences exhibited about 80% similarity for a small 31-amino-acid overlap of various ArrA sequences of Hollibaugh et al. (10). In both studies it was not clear what species the *arrA* sequences are affiliated with taxonomically.

Because the use of the *arrA* primers of Malasarn et al. (18) was limited, redesign of the primers with an archaeal codon bias resulted in significantly increased detection of *arrA*. To date, there are no known halophilic arsenate-respiring archaea in pure culture, although there are two hyperthermophilic archaea, *Pyrobaculum aerophilum* and *Pyrobaculum arsenaticum*, which respire arsenate. The genome sequence of *P. aerophilum* contains a distantly related homolog of *arrA*, which is undetectable using the primer set of Malasarn et al. (18). Moreover, the *P. aerophilum* ArrA-like sequence is a deeply branching homolog of bacterial ArrA sequences (Fig. 7). Whether the *arrA*-like sequences detected in ML and SL sediments had archaeal origins remains to be determined.

In summary, we determined pore water chemical profiles and in situ rates and employed molecular techniques to characterize dissimilatory arsenate reduction in the sediments of two anoxic soda lakes. The successful use of radiotracer in these systems could pave the way for using this technique to assess microbiologically driven arsenic mobilization in other types of sediments (e.g., freshwater ecosystems). Although drinking water aquifers are not as exotic as the extreme environments discussed here, the question of arsenic mobility in these aquifers is of vital concern to human health worldwide. In addition, a number of points that have basic scientific interest are also raised by our results, which may be pursued in future investigations. These include the cultivation of examples of extremely halophilic, anaerobic archaea that can respire As(V). With such isolates further insight into the degree of vertical genetic evolution versus horizontal genetic evolution

of the gene(s) for respiratory arsenate reductase could be obtained. There is also the challenge of characterizing As(III) oxidation in the sediments of these two lakes by using an interdisciplinary approach similar to the approach that we used in this study. Finally, there is the question of our detection of abundant cyanobacterial 16S rRNA gene sequences in the sediments of SL. Some attempt at estimating the importance of these organisms as primary producers would be of interest in order to learn more about the extent of carbon mineralization that can be attributed to arsenate respiration in this system, as was done previously for the anoxic water column of Mono Lake (9, 27). However, we also speculate about the possibility that the cyanobacterial strains may have a direct role in the arsenic cycle itself, either by carrying out resistance-based (e.g., ArsC) reduction of As(V) to As(III) or, conversely, by using As(III) as an electron donor to support anoxygenic photosynthesis.

ACKNOWLEDGMENTS

This work was funded in part by a NASA Exobiology grant to R.S.O. and by the U.S. Geological Survey.

REFERENCES

1. **Anderson, M. A., J. F. Ferguson, and J. Gavis.** 1975. Arsenate adsorption on amorphous aluminum hydroxide. J. Colloid Interface Sci. **54:**391–399.
2. **Andreae, M. O.** 1979. Arsenic speciation in seawater and interstitial waters: the influence of biological-chemical interactions on the chemistry of a trace element. Limnol. Oceanogr. **24:**440–452.
3. **Berner, R. A.** 1971. Principles of chemical sedimentology. McGraw Hill, New York, NY.
4. **Campos, V.** 2002. Arsenic in groundwater affected by phosphate fertilizers in Sao Paulo, Brazil. Environ. Geol. **42:**83–87.
5. **Cherry, J. A., A. U. Shaikh, D. E. Tallman, and R. V. Nicholson.** 1979. Arsenic species as an indicator of redox conditions in groundwater. J. Hydrol. **43:**373–392.
6. **Cline, J. D.** 1969. Spectrophotometric determination of hydrogen sulfide in natural waters. Limnol. Oceanogr. **14:**454–459.
7. **Coolen, M. J. L., E. C. Hopmans, W. I. C. Rijpstra, G. Muyzer, S. Schouten, J. K. Volkman, and J. S. Sinninghe Damste.** 2004. Evolution of the methane cycle in Ace Lake (Antarctica) during the Holocene: response of methanogens and methanotrophs to environmental change. Org. Geochem. **34:**1151–1167.
8. **Hoeft, S. E., T. R. Kulp, J. F. Stolz, J. T. Hollibaugh, and R. S. Oremland.** 2004. Dissimilatory arsenate reduction with sulfide as an electron donor: experiments with Mono Lake water and isolation of strain MLMS-1, a chemoautotrophic arsenate respirer. Appl. Environ. Microbiol. **70:**2741–2747.
9. **Hollibaugh, J. T., S. Carini, H. Gürleyuk, R. Jellison, S. B. Joye, G. LeCleir, C. Meile, L. Vasquez, and D. Wallschlager.** 2005. Arsenic speciation in Mono Lake, California: response to seasonal stratification and anoxia. Geochim. Cosmochim. Acta **69:**1925–1937.
10. **Hollibaugh, J. T., C. Budinoff, R. A. Hollibaugh, B. Ransom, and N. Bano.** 2006. Sulfide oxidation coupled to arsenate reduction by a diverse microbial community in a soda lake. Appl. Environ. Microbiol. **72:**2043–2049.
11. **Jellison, R., and J. M. Melack.** 1993. Meromixis in hypersaline Mono Lake, California. 1. Stratification and vertical mixing during the onset, persistence, and breakdown of meromixis. Limnol. Oceanogr. **38:**1008–1019.
12. **Joye, S. B., A. Boetius, B. N. Orcutt, J. P. Montoya, H. N. Schulz, M. J. Erickson, and S. K. Lugo.** 2004. The anaerobic oxidation of methane and sulfate reduction in sediments from Gulf of Mexico cold seeps. Chem. Geol. **205:**219–238.
13. **Keon, N. E., C. H. Swartz, D. J. Brabander, C. Harvey, and H. F. Hemond.** 2001. Validation of an arsenic sequential extraction method for evaluating mobility in sediments. Environ. Sci. Technol. **35:**2778–2784.
14. **Kneebone, P. E., P. A. O'Day, N. Jones, and J. G. Hering.** 2002. Deposition and fate of arsenic in iron- and arsenic-enriched reservoir sediments. Environ. Sci. Technol. **36:**381–386.
15. **Kulp, T. R., S. E. Hoeft, and R. S. Oremland.** 2004. Redox transformations of arsenic oxyanions in periphyton communities. Appl. Environ. Microbiol. **70:**6428–6434.
16. **Li, Y. H., and S. Gregory.** 1974. Diffusion of ions in sea water and in deep-sea sediments. Geochim. Cosmochim. Acta **38:**703–714.
17. **Macy, J. M., J. M. Santini, B. V. Pauling, A. H. O'Neill, and L. I. Sli.** 2000. Two new arsenate/sulfate-reducing bacteria: mechanisms of arsenate reduction. Arch. Microbiol. **173:**49–57.
18. **Malasarn, D., C. W. Saltikov, K. M. Campbell, J. M. Santini, J. G. Hering, and D. K. Newman.** 2004. *arrA* is a reliable marker for As(V) respiration. Science **306:**455.
19. **Manning, B. A., and D. A. Martens.** 1997. Speciation of arsenic(III) and arsenic(V) by high performance liquid chromatography-hydride generation atomic absorption spectrophotometry. Environ. Sci. Technol. **31:**171–177.
20. **Marvin-DiPasquale, M., A. Oren, Y. Cohen, and R. S. Oremland.** 1998. Radiotracer studies of bacterial methanogenesis in sediments from the Dead Sea and Solar Lake (Sinai), p. 135–149. *In* A. Oren (ed.), Microbiology and biogeochemistry of hypersaline environments. CRC Press, Boca Raton, FL.
21. **Miller, L. G., R. Jellison, R. S. Oremland, and C. W. Culbertson.** 1993. Meromixis in hypersaline Mono Lake, California. 3. Biogeochemical response to stratification and overturn. Limnol. Oceanogr. **38:**1040–1051.
22. **Mucci, A., L. F. Richard, M. Lucotte, and C. Guignard.** 2000. The differential geochemical behavior of arsenic and phosphorous in the water column and sediments of the Saguenay Fjord Estuary, Canada. Aquat. Geochem. **6:**293–324.
23. **Muyzer, G., E. C. De Waal, and A. G. Uitterlinden.** 1993. Profiling of complex populations by denaturing gradient gel electrophoresis analysis of polymerase chain reaction-amplified genes coding for 16S rRNA. Appl. Environ. Microbiol. **59:**695–700.
24. **Newman, D. K., E. K. Kennedy, J. D. Coates, D. Ahmann, D. J. Ellis, D. R. Lovely, and F. M. M. Morel.** 1997. Dissimilatory arsenate and sulfate reduction in *Desulfotomaculum auripigmentum* sp. nov. Arch. Microbiol. **168:**380–388.
25. **Nordstrom, D. K.** 2002. Worldwide occurrences of arsenic in ground water. Science **296:**2143–2144.
26. **Oremland, R. S.** 1990. Nitrogen fixation dynamics of two diazotrophic communities in Mono Lake, California. Appl. Environ. Microbiol. **56:**614–622.
27. **Oremland, R. S., P. R. Dowdle, S. Hoeft, J. O. Sharp, J. K. Schaefer, L. G. Miller, J. Switzer-Blum, R. L. Smith, N. S. Bloom, and D. Wallschlaeger.** 2000. Bacterial dissimilatory reduction of arsenate and sulfate in meromictic Mono Lake, California. Geochim. Cosmochim. Acta **64:**3073–3084.
28. **Oremland, R. S., S. E. Hoeft, J. M. Santini, N. Bano, R. A. Hollibaugh, and J. T. Hollibaugh.** 2002. Anaerobic oxidation of arsenite in Mono Lake water and by a facultative, arsenite-oxidizing chemoautotroph, strain MLHE-1. Appl. Environ. Microbiol. **68:**4795–4802.
29. **Oremland, R. S., T. R. Kulp, J. Switzer-Blum, S. E. Hoeft, S. Baesman, L. G. Miller, and J. Stolz.** 2005. A microbial arsenic cycle in a salt-saturate, extreme environment. Science **308:**1305–1308.
30. **Oremland, R. S., and L. G. Miller.** 1993. Biogeochemistry of natural gases in three alkaline, permanently stratified (meromictic) lakes, p. 439–452. *In* D. G. Howell (ed.), The future of energy gases. U.S. Geological Survey, Menlo Park, Calif.
31. **Oremland, R. S., N. A. Steinberg, A. S. Maest, L. G. Miller, and J. T. Hollibaugh.** 1990. Measurement of in situ rates of selenate removal by dissimilatory bacterial reduction in sediments. Environ. Sci. Technol. **24:**1157–1164.
32. **Oremland, R. S., and J. F. Stolz.** 2003. The ecology of arsenic. Science **300:**939–944.
33. **Oremland, R. S., and J. F. Stolz.** 2005. Arsenic, microbes and contaminated aquifers. Trends Microbiol. **13:**45–49.
34. **Oremland, R. S., J. F. Stolz, and J. T. Hollibaugh.** 2004. The microbial arsenic cycle in Mono Lake, California. FEMS Microbiol. Ecol. **48:**15–27.
35. **Oren, A.** 1999. Bioenergetic aspects of halophilism. Microbiol. Mol. Biol. Rev. **63:**334–348.
36. **Peterson, M. L., and R. Carpenter.** 1983. Biogeochemical processes affecting total arsenic and arsenic species distributions in an intermittently anoxic fjord. Mar. Chem. **12:**295–321.
37. **Pierce, M. L., and C. B. Moore.** 1982. Adsorption of arsenite and arsenate on amorphous iron hydroxide. Water Res. **16:**1247–1253.
38. **Reimer, K. J., and J. A. J. Thompson.** 1988. Arsenic speciation in marine interstitial water. The occurrence of organoarsenicals. Biogeochemistry **6:**211–237.
39. **Rochette, E. A., B. C. Bostick, G. Li, and S. Fendorf.** 2000. Kinetics of arsenate reduction by dissolved sulfide. Environ. Sci. Technol. **34:**4714–4720.
40. **Senn, D. B., and H. F. Hemond.** 2002. Nitrate controls on iron and arsenic in an urban lake. Science **296:**2373–2376.
41. **Seyler, P., and J. M. Martin.** 1989. Biogeochemical processes affecting arsenic species distribution in a permanently stratified lake. Environ. Sci. Technol. **23:**1258–1263.
42. **Skidmore, M., S. P. Anderson, M. Sharp, J. M. Foght, and B. D. Lanoil.** 2005. Comparison of microbial community compositions of two subglacial environments reveals a possible role for microbes in chemical weathering processes. Appl. Environ. Microbiol. **71:**6986–6997.
43. **Smedley, P. L., and D. G. Kinniburgh.** 2002. A review of the source, behaviour and distribution of arsenic in natural waters. Appl. Geochem. **17:**517–568.
44. **Smith, A. H., E. O. Lingas, and M. Rahman.** 2000. Contamination of drinking water by arsenic in Bangladesh: a public health emergency. Bull. W. H. O. **78:**1093–1103.

45. **Solórzano, L.** 1969. Determination of ammonia in natural waters by the phenolhypochlorite method. Limnol. Oceanogr. **14:**799–801.
46. **Sullivan, K. A., and R. C. Aller.** 1996. Diagenetic cycling of arsenic in Amazon shelf sediments. Geochim. Cosmochim. Acta **60:**1465–1477.
47. **Takamatsu, T., M. Kawashima, and M. Koyama.** 1985. The role of Mn^{2+}-rich hydrous manganese oxide in the accumulation of arsenic in lake sediments. Water Res. **19:**1029–1032.
48. **Ullman, W. J., and R. C. Aller.** 1982. Diffusion coefficients in nearshore marine sediments. Limnol. Oceanogr. **27:**552–556.
49. **Widdel, F., G. W. Kohring, and F. Mayer.** 1983. Studies on dissimilatory sulfate-reducing bacteria that decompose fatty acids. III. Characterization of the filamentous gliding *Desulfonema limicola* gen. nov. sp. nov., and *Desulfonema magnum* sp. nov. Arch. Microbiol. **134:**286–294.
50. **Wilkin, R. T., D. Wallschläger, and R. G. Ford.** 2003. Speciation of arsenic in sulfidic waters. Geochem. Trans. **4:**1–7.
51. **Yano, Y., T. Miyama, A. Ito, and T. Yasuda.** 2000. Convenient measurements and speciation of arsenic in water by use of simple pretreatments for atomic absorption spectrometry in combination with hydride generation. Anal. Sci. **16:**939–943.
52. **Ye, Q., Y. Roh, S. L. Carroll, B. Blair, J. Zhou, C. L. Zhang, and M. W. Fields.** 2004. Alkaline anaerobic respiration: isolation and characterization of a novel alkaliphilic and metal-reducing bacterium. Appl. Environ. Microbiol. **70:**5595–5602.
53. **Zobrist, J., P. R. Dowdle, J. A. Davis, and R. S. Oremland.** 2000. Mobilization of arsenite by dissimilatory reduction of adsorbed arsenate. Environ. Sci. Technol. **34:**4747–4753.